Model Testing of the Wave Energy Converter Seawave Slot-Cone Generator

Kofoed, Jens Peter

Publication date:
2005

Document Version
Publisher's PDF, also known as Version of record

AALBORG UNIVERSITY

Model testing of the wave energy converter Seawave Slot-Cone Generator

according to Co-operation Agreement between
WAVEenergy (Norway) and Aalborg University, Dept. of Civil Engineering

Jens Peter Kofoed, Aalborg University

April, 2005

Department of Civil Engineering
Aalborg University - Sohngaardsholmsvej 57 - DK 9000 Aalborg - Telephone +45 9635 8080

DEPARTMENT OF CIVIL ENGINEERING
AALBORG UNIVERSITY
SOHNGAARDSHOLMSVEJ 57 DK-9000 AALBORG DENMARK
TELEPHONE +45 96 35 80 80 TELEFAX +45 98 14 25 55

Hydraulics and Coastal Engineering No. 18

ISSN: 1603-9874

Model testing of the wave energy converter Seawave Slot-Cone Generator

By

Jens Peter Kofoed, Aalborg University

April, 2005

Preface

This report presents the results of a preliminary experimental study of the wave energy convert (WEC) Seawave Slot-Cone Generator (SSG). SSG is a WEC utilizing wave overtopping in multiple reservoirs. In the present SSG setup three reservoirs has been used.

Model tests have been performed using a scale model (length scale 1:15) of a SSG device to be installed on the west coast of the island Kvitsøy near Stavanger, Norway. The tests were carried out at Dept. of Civil Engineering, Aalborg University (AAU) in the 3D deep water wave tank. The model has been subjected to regular and irregular waves corresponding to typical conditions off shore from the intended installation site. The overtopping rates for the individual reservoirs have been measured and the potential energy in the overtopping water has been calculated.

The tests have been performed by Jens Peter Kofoed, AAU, in co-operation with Espen Osaland, WAVEenergy, Norway (WE), who was present in the laboratory during the tests. The testing took place during the period 21-24/2, 2005. The report has been prepared by Jens Peter Kofoed (tlf.: +45 9635 8474, e-mail: i5jpk@civil.aau.dk).

The work has been carried out according to a Co-operation Agreement between WAVEenergy (Norway) and Aalborg University, Dept. of Civil Engineering.

Aalborg, April, 2005.

Table of Contents

1 Introduction

The purpose of the work described in the present report has been to check the applicability of model tests using regular waves performed by WE in their in-house built wave test/demonstration facility and to test various geometrical layouts of the SSG structure in irregular sea, quantify the obtained potential energy in the overtopping water captured in the three reservoirs, and thereby if possible provide guidelines on how to optimize the structure in terms of maximizing the obtained potential energy.

AAU has considerable experience in the field of testing WEC's based on the overtopping principle. Most relevant is the former work done on the WEC Wave Dragon (see e.g. Kofoed, 2004), the WEC Power Pyramid (see Kofoed, 2002b) and the more generic study on wave overtopping, Kofoed (2002).

2 Model test setup

The model tests have been performed in the 3D-deep water wave tank at AAU. Although the wave making facility in the used wave tank is capable of producing 3-D wave conditions, on 2-D regular and irregular wave conditions have been applied. The setup primarily consists of 3 components, see Figure 1:

- Leading walls (with a distance equal to the width of the test section, 0.5 m, model scale) installed in front of the test section, in order to have well defined 2-D incoming waves. The incoming waves are measured by three wave gauges placed be between the leadings walls (in the hereby established flume) in front of the test section. Furthermore, a single wave gauge was deployed outside the flume, allowing for comparisons.
- The test section it self. The initial geometry has been provided by WE, but the test section has been constructed so modification here of could relatively easy could be made. The geometrical layout of the tested sections are described in The three reservoirs were connected by large dimension hoses to reservoir tanks outside the wave tank.
- Reservoir tanks. Each of the three reservoirs in the test section has a reservoir tank which is used to measure the amount of overtopping in the individual reservoir. In each reservoir tank a level gauge and a pump was placed. The level gauge and the pump were connected to a PC programmed to emptying the reservoir tanks and thereby recording the amount of overtopping water in the individual reservoirs.

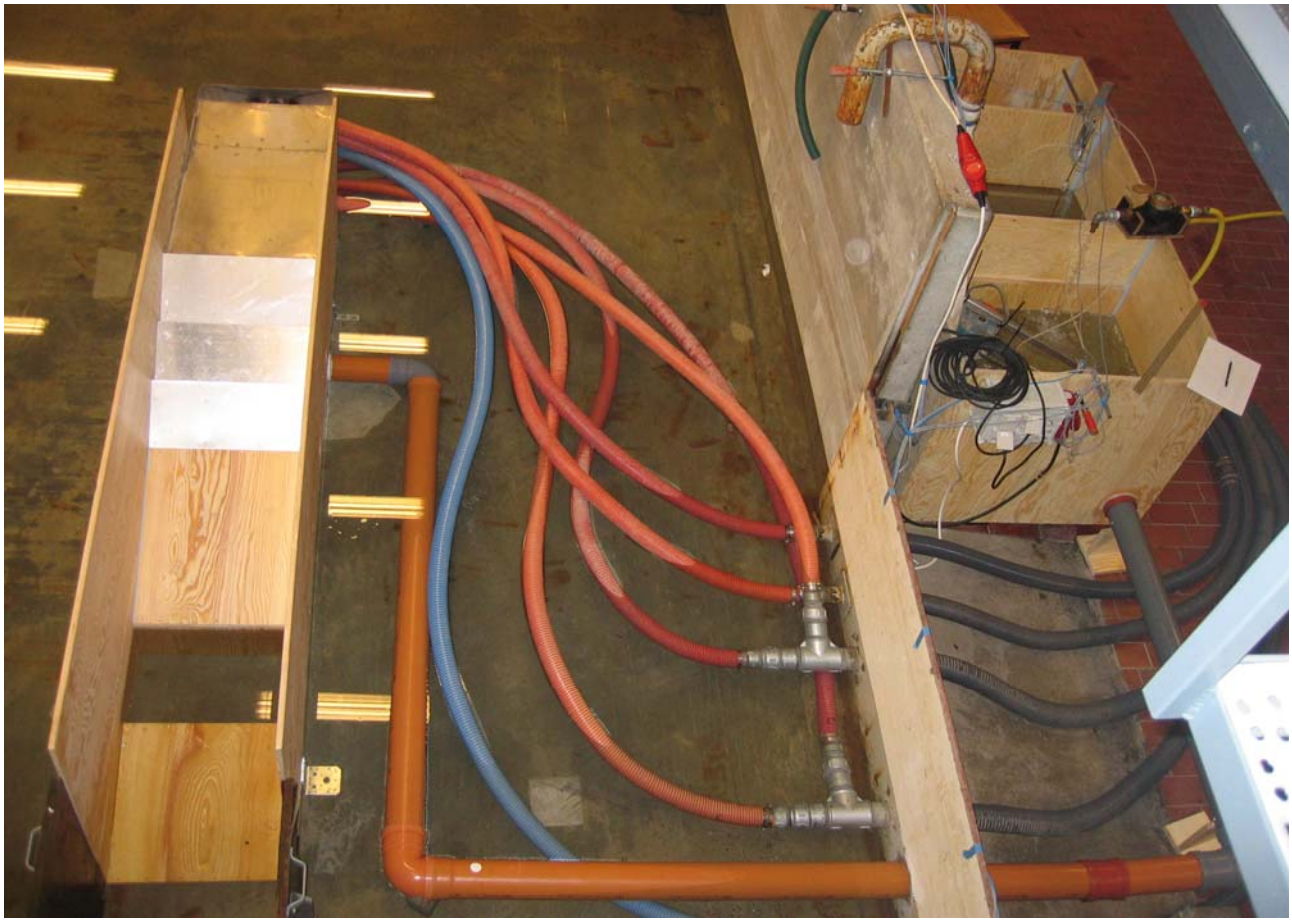

Figure 1. Model test setup.

Prior to the testing the wave gauge, level gauges, volume of reservoir tanks and pump capacities have been calibrated.

2.1 Tested geometries

A total of 10 geometries have been tested. All tests have been performed with a water depth d = 0.4 m (6 m full scale) and ramp angles of 35° on all reservoir fronts. The initial geometry is shown in Figure 2. The 10 geometries are described below:

- Geometry A: Slope angle of 19°. Crest level of reservoir 1 (lower), 2 (middle) and 3 (upper) is $R_{c,1}$ = 0.15 m (2.25 m full scale, $R_{c,1}/d$ = 0,375), $R_{c,2}$ = 0.22 m (3.30 m full scale, $R_{c,2}/d$ = 0,55) and $R_{c,3}$ = 0.31 m (4,65 m full scale, $R_{c,3}/d$ = 0,775), respectively. Four variations of this layout has been used:
  - A1: Slope cut off vertically at 0.25 m (3,75 m full scale, 0.625 d) above the bottom.
  - A2: Slope cut off vertically at 0.20 m (3.00 m full scale, 0.5 d) above the bottom.
  - A3: Slope cut off vertically at 0.15 m (2.25 m full scale, 0.375 d) above the bottom.
  - A4: Slope extending all the way to the bottom.
- Geometry C: As A4, but with a slope angle of 35°.
- Geometry D: As A4, but with a slope angle of 30°.
- Geometry D2: As D, but with reservoir fronts on reservoir 2 and 3 cut off at the crest level of the reservoir below. Distance from crest of reservoir 1 to lower edge of reservoir 2 is 0.087 m (1.30 m full scale). Distance from crest of reservoir 2 to lower edge of reservoir 3 is 0.087 m (1.30 m full scale).
- Geometry D3: As D2, but with distance from crest of reservoir 1 to lower edge of reservoir 2 reduced to 0.06 m (0.90 m full scale). Distance from crest of reservoir 2 to lower edge of reservoir 3 reduced to 0.04 m (0.60 m full scale).
- Geometry E: As D, but with $R_{c,1}$ = 0.10 m (1.50 m full scale, $R_{c,1}/d$ = 0,25).
- Geometry E2: As E, but with front on reservoir 2 extended so the lover edge of it reaches the relative position to the crest of reservoir 1 as in A – D (0.05 m (0.75m full scale) from the crest of reservoir 1 in the direction perpendicular to the front).

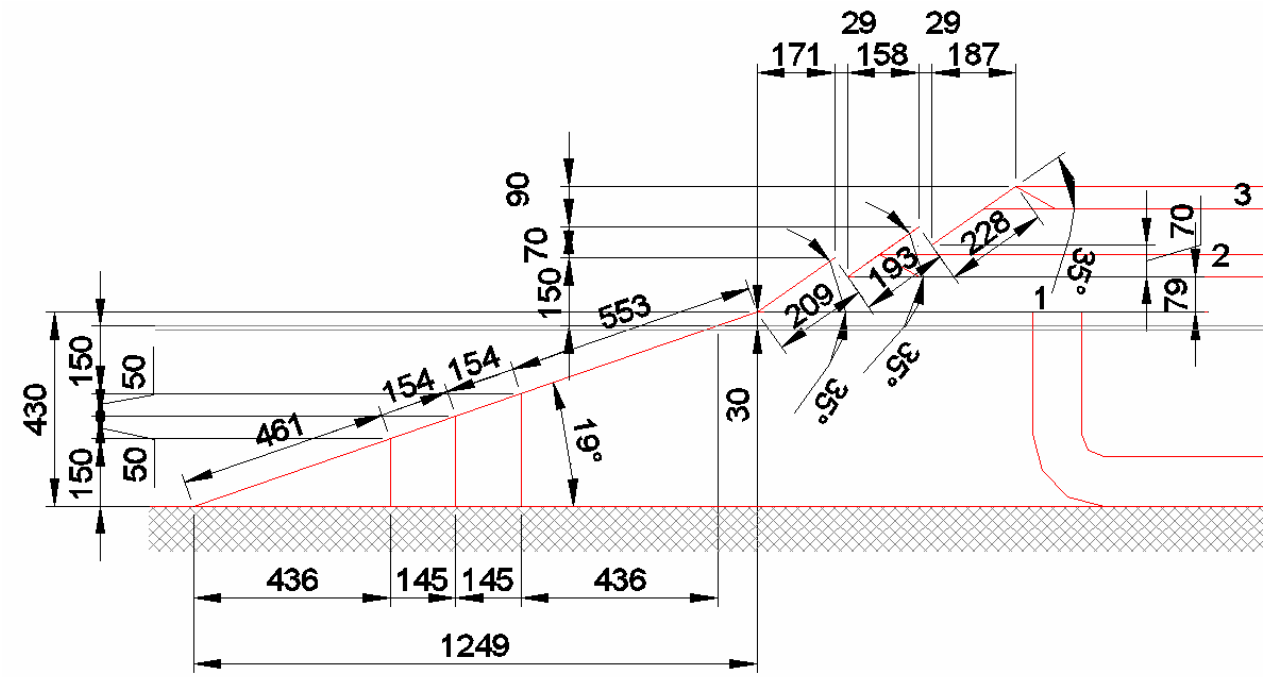

Figure 2. Geometry A1-4. A4 is the geometry shown, with all parts of the slope extending to the bottom. Geometry A3, A2 and A1 is obtained by removing the indicated slope sections from sea side, resulting in cutting of the slope vertically. Measures are in mm, model scale.

2.2 Wave conditions

From Vind- og temperaturstatistikk, DNMI, for Utsira during the period 1961-1990, Table 1 has been established in order to roughly describe the wave climate offshore from the planned location of deployment of the prototype SSG on the west coast of Kvitsøy. Utsira is an island located roughly 50 km north-west of Kvitsøy. Vind- og temperaturstatistikk, DNMI, does not provide any information about the wave periods and therefore the wave peak period T_p has been estimated for the individual 1 m ranges for the significant wave height H_s as

$$T_p = \sqrt{\frac{245 H_s}{g}}$$

This relation is used based on a recommendation of an interval for the wave period T from DS 449, 1983

$$\sqrt{\frac{130 H_s}{g}} < T < \sqrt{\frac{280 H_s}{g}}$$

The choice of $T_p - H_s$ relation is based on an expectation of the wave periods being slightly larger in southern Norwegian part of the North Sea than in the Danish part, for which DS 449 is intended. Furthermore, the resulting wave periods have been found to be comparable to findings by Torsethaugen, 1990.

Also the energy period T_e has been estimated – here simply set to be $T_p/1.15$. Finally, the wave energy transport has been found by

$$P_{wave} = \frac{\rho g^2}{64\pi} T_e H_s^2$$

as given by Falnes, 1993.

Hs [m]	0-1	1-2	2-3	3-4	4-5	5-6	6-7	7-8	8-9	9-10
jan	6	18	25	23	15	8	3	1	1	0
feb	11	22	26	21	12	5	2	1	0	0
mar	8	23	26	22	12	6	2	1	0	0
apr	17	33	27	14	6	2	1	0	0	0
may	24	41	23	7	3	1	1	0	0	0
jun	24	42	23	9	2	0	0	0	0	0
jul	19	48	25	7	1	0	0	0	0	0
aug	22	45	25	6	2	0	0	0	0	0
sep	10	32	33	16	6	2	1	0	0	0
oct	6	25	30	22	10	4	2	1	0	0
nov	4	19	30	25	13	6	2	1	0	0
dec	4	16	25	25	17	8	4	1	0	0
Prob. [%]	**12.9**	**30.3**	**26.5**	**16.4**	**8.3**	**3.5**	**1.5**	**0.5**	**0.1**	**-**
Hs	**0.5**	**1.5**	**2.5**	**3.5**	**4.5**	**5.5**	**6.5**	**7.5**	**8.5**	**9.5**
Tp	**3.5**	**6.1**	**7.9**	**9.3**	**10.6**	**11.7**	**12.7**	**13.7**	**14.6**	**15.4**
Te [s]	3.07	5.32	6.87	8.13	9.21	10.19	11.07	11.89	12.66	13.39
Pwave [kW/m]	**0.38**	**5.86**	**21.03**	**48.77**	**91.42**	**150.98**	**229.25**	**327.85**	**448.30**	**592.02**

Table 1. Probability of significant wave heights (H_s) within the given 1 m ranges for the individual months of the year, based on Vind- og temperaturstatistikk, DNMI, for Utsira during the period 1961-1990. The overall probability for the 1 m significant wave height ranges are given, along with estimated wave peak periods (T_p) and wave energy transport (or available wave power) (P_{wave})

For the performed tests the wave conditions covered by the significant wave height range 1 – 5 m have been chosen, as these conditions covers 81.5 % of the time, and 78.4 % of the available energy. The average P_{wave} of all the wave conditions is 33.7 kW/m, while the average P_{wave} in the 1 – 5 m range is 28.1 kW/m.

As mentioned, the wave conditions given in Table 1 are valid for offshore conditions, meanwhile the tested structure is to be placed at very shallow water. However, no analyses of the transformation of the waves from offshore to the prototype location have been available or

performed. The seabed topography going from offshore to location can roughly be described as follows: A few hundred meters offshore the seabed rise steeply from a depth of >150 m and to 30-40 m, and this gradually goes down to ~25 m close to shore. The seabed then rapidly rises again to the water depth of 6 m where prototype will be placed.

Obviously, a significant amount of the waves will break on their way to the location of the prototype, but in the lack of an analysis of the transformation, the offshore wave parameters have been used as input in the wave generation in the wave tank, and then wave breaking occurs before and on the structure in the model test. This entails that the target offshore wave conditions can not be reproduced in the model test at the shallow water where the prototype is placed.

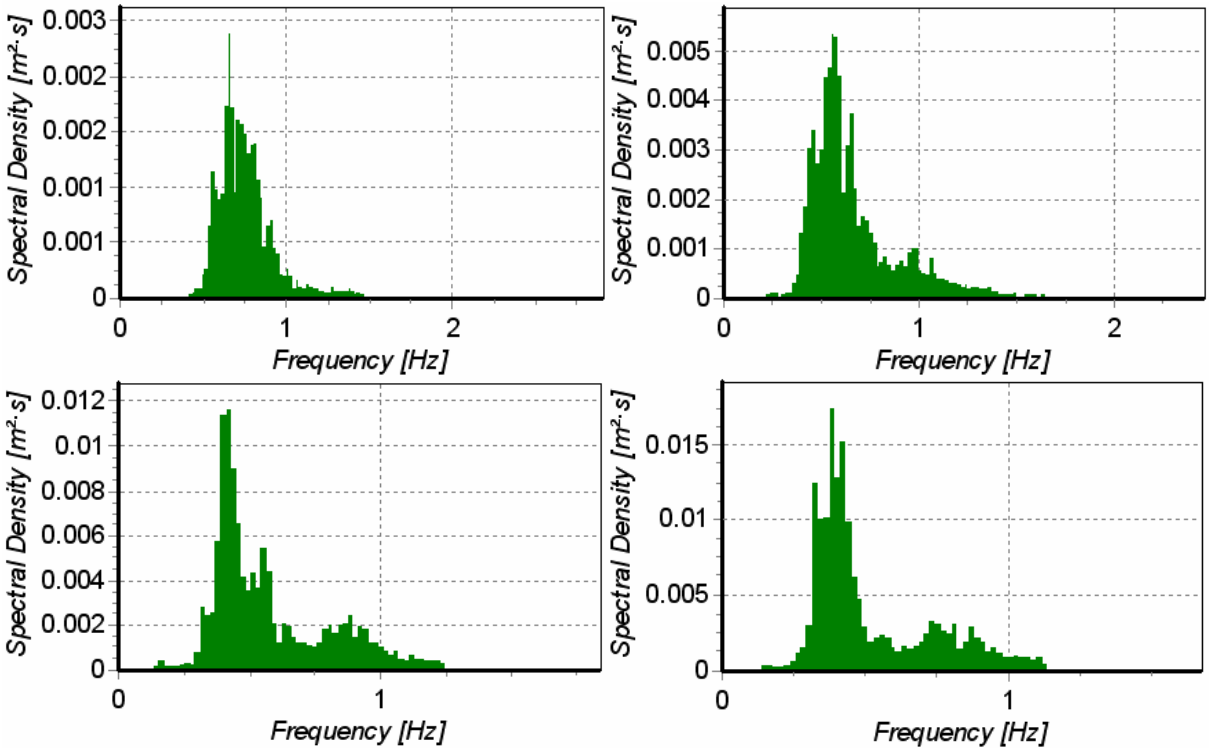

Figure 3. Measured wave spectra from the model tests for the four wave conditions (upper left: 1-2, upper right: 2-3, lower left: 3-4, lower right: 4-5) used in the wave tank. It is seen that the higher the offshore wave heights, the more wave breaking is occuring, which is seen as spectral energy is moved to higher frequencies, concentrated around 2 f_p.

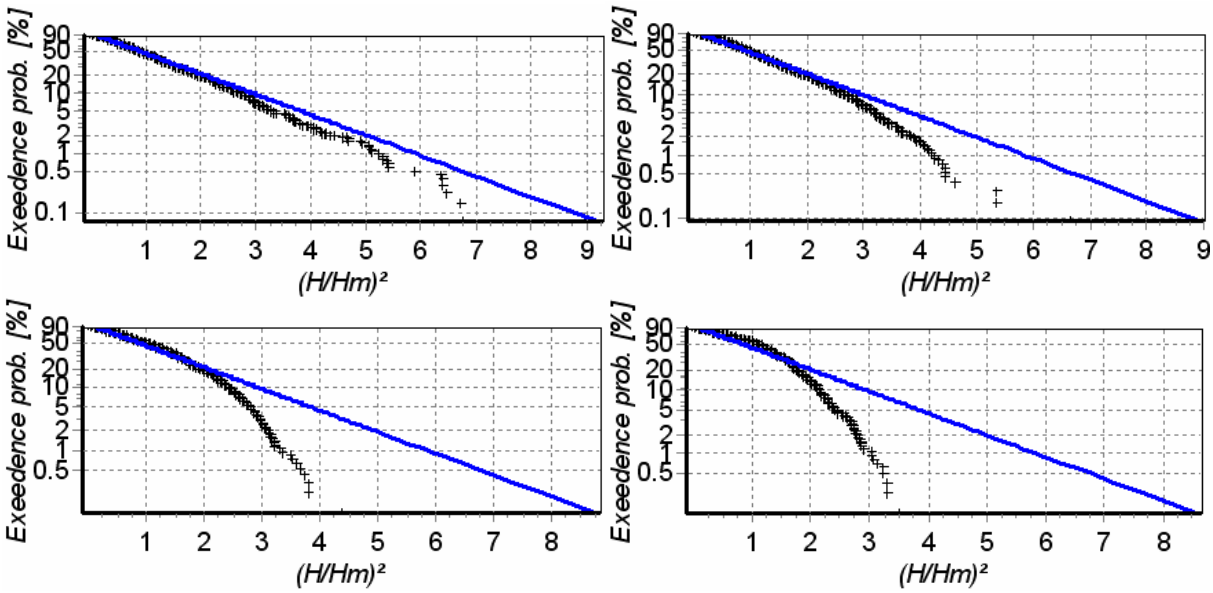

Figure 4. Measured wave height distributions from the model tests for the four wave conditions (upper left: 1-2, upper right: 2-3, lower left: 3-4, lower right: 4-5) used in the wave tank. It is seen that the higher the offshore wave heights, the more wave breaking is occuring, which is seen as the measured wave height distributions deviated more and more from the Rayleigh distribution (the straight blue lines) with increasing wave conditions.

Wave cond.	1-2	2-3	3-4	4-5
Hs [m]	1.50	2.50	3.50	4.50
Tp [s]	6.1	7.9	9.3	10.6
Hs, realized [m]	1.54	2.25	2.80	3.35
Pwave, realized [kW/m]	6.2	17.1	31.2	50.9
Prob. [%]	30.3	26.5	16.4	8.3

Table 2. Generated and realized (measured in front of tested structure, full scale values) wave conditions and corresponding available wave power.

In Table 2 the wave conditions generated in the laboratory is given along with the realized (measured) wave conditions on the shallow water corresponding to the location of the prototype.

The average of P_{wave} for the realized wave conditions (1-5) at location of the prototype in the model tests is 19.3 kW/m, i.e. a decrease of 31 % compared to offshore. However, it should be noted that in the used expression for P_{wave} is not completely applicable on the shallow water conditions where the wave height distribution and spectra shapes differs significantly from the normal deep water situations due to heavy wave breaking.

Most of the tested geometries have been subjected to irregular waves corresponding to the 4 wave conditions given in Table 2. The duration of each of the tests performed with irregular waves was 30 min. corresponding to approx. 2 hours in full scale.

A few tests with regular waves were also performed for a few of the geometries. The duration of these tests were 5 min. The generated waves are given in Table 3.

Wave cond.	2-3	3-4	4-5
H [m]	1.77	2.48	3.18
T [s]	7.9	9.3	10.6
Prob. [%]	26.5	16.4	8.3

Table 3. Wave parameters (prototype scale) used for regular waves model tests.

However, after running a few tests with regular waves, it was concluded that the results hereof were hardly useful because, although the wave parameters for the regular waves have been selected so the amount of energy corresponds to the irregular wave condition, the overtopping rates obtained from the regular waves model tests are not representing the overtopping rates for the irregular waves occurring in nature. This is due to the following:

- Wave overtopping is a highly non-linear process, and reproduction of the individual waves in the irregular wave train is important and cannot be replaced by just looking at a single wave without considerable loss of accuracy.
- When running regular waves, resonance effects arise on the ramp of the structure. This can be both destructive and constructive, but will not occur to near the same extend in irregular waves.
- The location of nodes and anti-nodes due to reflection from the structure is constant when only one wave length is present, as is the case with regular waves. This means that the exact placement of the tested structure and the wave gauges becomes very important, and the results will change if the placements are changed.

For these reasons further testing using regular waves were abandoned. It was also found that the tendencies found from the tests performed by WE in Norway could not be reproduced, and it was there chosen to focus on performing the model tests using irregular waves.

3 Results of performed model tests

A total of 31 model tests have been performed using irregular 2-D waves. In Table 4 the results of the model tests are presented in terms of full scale overtopping rates (q_n, n indicating the reservoir number) and hydraulic power in each of the three reservoirs (P_n, n, found as the overtopping rate times the crest freeboard of the reservoir times the acceleration of gravity), and the total overtopping rate (q_{total}, the sum of q_n) and total hydraulic power (P_{total}, the sum of P_n) and efficiency (defined as the ratio between P_{total} and P_{wave}) for the individual tests. Furthermore, the same data has been plotted in Figure 5 to Figure 10.

Geometry	Wave cond.	q1 [m^3/s/m]	q2 [m^3/s/m]	q3 [m^3/s/m]	P1 [kW/m]	P2 [kW/m]	P3 [kW/m]	Ptotal [kW/m]	eff. [-]
A1	2-3	0.121	0.045	0.014	2.74	1.50	0.63	4.88	0.285
	3-4	0.180	0.103	0.060	4.07	3.43	2.80	10.30	0.330
	4-5	0.208	0.139	0.114	4.72	4.63	5.32	14.67	0.288
A2	2-3	0.119	0.042	0.014	2.69	1.39	0.65	4.74	0.277
	3-4	0.204	0.110	0.069	4.62	3.66	3.23	11.51	0.368
	4-5	0.223	0.140	0.109	5.05	4.64	5.09	14.77	0.290
A3	2-3	0.129	0.048	0.015	2.93	1.59	0.72	5.24	0.307
	3-4	0.200	0.114	0.075	4.54	3.80	3.51	11.84	0.379
	4-5	0.235	0.145	0.134	5.32	4.81	6.29	16.43	0.323
A4	1-2	0.025	0.006	0.001	0.57	0.19	0.03	0.79	0.127
	2-3	0.118	0.046	0.020	2.68	1.53	0.93	5.14	0.301
	3-4	0.185	0.105	0.074	4.18	3.50	3.44	11.13	0.356
	4-5	0.233	0.154	0.143	5.28	5.10	6.68	17.07	0.336
C	1-2	0.021	0.002	0.000	0.49	0.07	0.00	0.56	0.090
	2-3	0.121	0.036	0.013	2.74	1.20	0.61	4.55	0.266
	3-4	0.182	0.105	0.064	4.12	3.50	3.02	10.64	0.341
	4-5	0.227	0.139	0.111	5.14	4.61	5.19	14.93	0.294
D	1-2	0.030	0.004	0.000	0.69	0.12	0.01	0.82	0.132
	2-3	0.118	0.039	0.015	2.68	1.30	0.71	4.69	0.275
	3-4	0.180	0.099	0.061	4.07	3.27	2.85	10.20	0.326
	4-5	0.229	0.139	0.124	5.20	4.63	5.82	15.64	0.308
D2	1-2	0.034	0.004	0.000	0.76	0.12	0.02	0.90	0.146
	2-3	0.130	0.031	0.009	2.94	1.03	0.42	4.40	0.258
	3-4	0.207	0.086	0.052	4.69	2.84	2.44	9.98	0.319
	4-5	0.238	0.121	0.099	5.39	4.03	4.61	14.03	0.276
D3	1-2	0.022	0.003	0.000	0.49	0.10	0.02	0.60	0.098
	2-3	0.123	0.040	0.020	2.79	1.34	0.95	5.08	0.298
	3-4	0.190	0.093	0.067	4.30	3.10	3.15	10.55	0.338
	4-5	0.225	0.121	0.121	5.10	4.01	5.68	14.78	0.291
E	1-2	0.085	0.004	0.001	1.28	0.13	0.03	1.44	0.233
	2-3	0.272	0.037	0.013	4.10	1.24	0.61	5.94	0.348
	3-4	0.367	0.097	0.059	5.55	3.23	2.75	11.52	0.369
E2	2-3	0.186	0.045	0.014	2.81	1.50	0.66	4.97	0.291

Table 4. Results of performed model tests in terms of full scale overtopping rates and hydraulic power in the three reservoirs, and the total power and efficiency, for the individual tests.

Also the overall efficiencies for the geometries have been calculated as the ratio $\Sigma P_{total} \cdot Prob$ / $\Sigma P_{wave} \cdot Prob$ for the considered wave conditions. In Table 5 these overall efficiencies are given for 3 different combinations of wave conditions, in order to facilitate comparison although not all geometries have been subjected to all wave conditions.

Geometry	Eff. (1-4) [-]	**Eff. (1-5) [-]**	Eff. (2-5) [-]
A1			0.303
A2			0.315
A3			0.339
A4	0.297	0.307	0.332
C	0.271	0.277	0.302
D	0.274	0.283	0.304
D2	0.267	0.269	0.286
D3	0.283	0.285	0.310
E	0.338	(0.342)	(0.356)
E2			

Table 5. Overall efficiencies. The ranges in the brackets refer to the wave conditions. Figures in brackets for geometry E are extrapolated values, see details in Chapter 5.

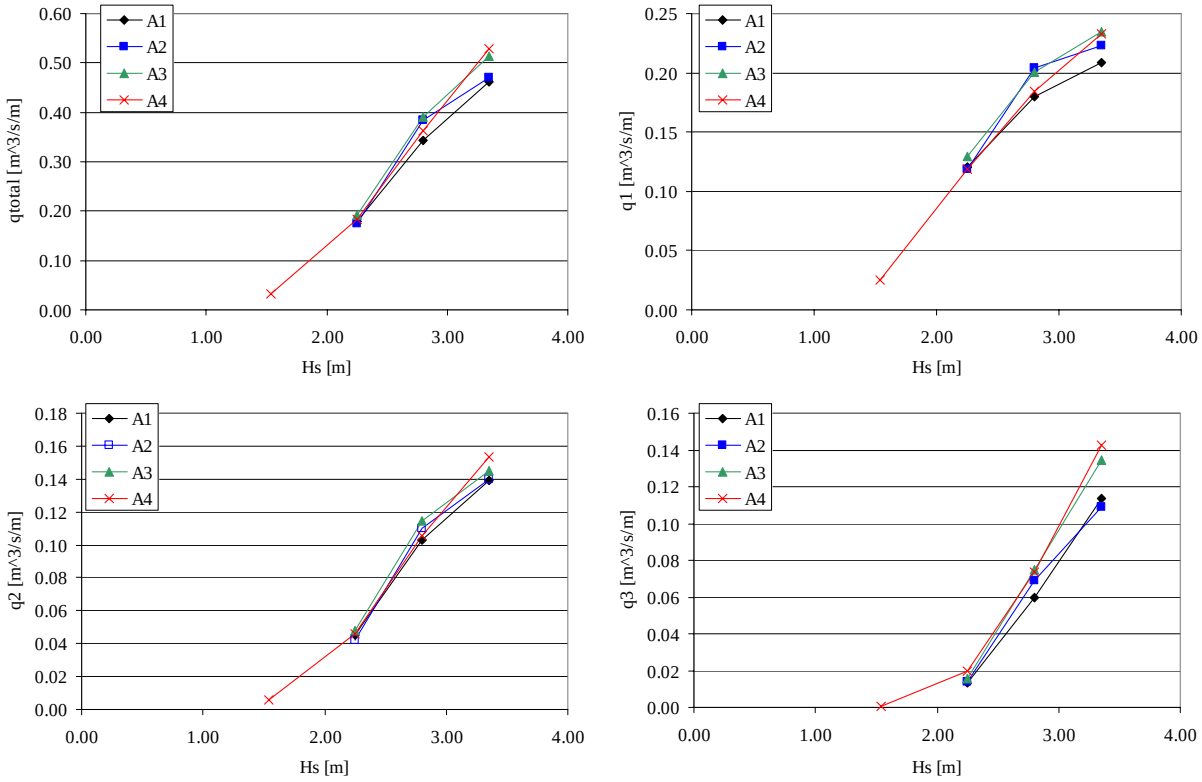

Figure 5. Geometries A1-4, length of slope in front of structure varied. Upper left: Total overtopping rate as a function of wave condition. Upper right: Overtopping rate for reservoir 1 as a function of the wave condition. Lower left: Overtopping rate for reservoir 2 as a function of the wave condition. Lower right: Overtopping rate for reservoir 3 as a function of the wave condition.

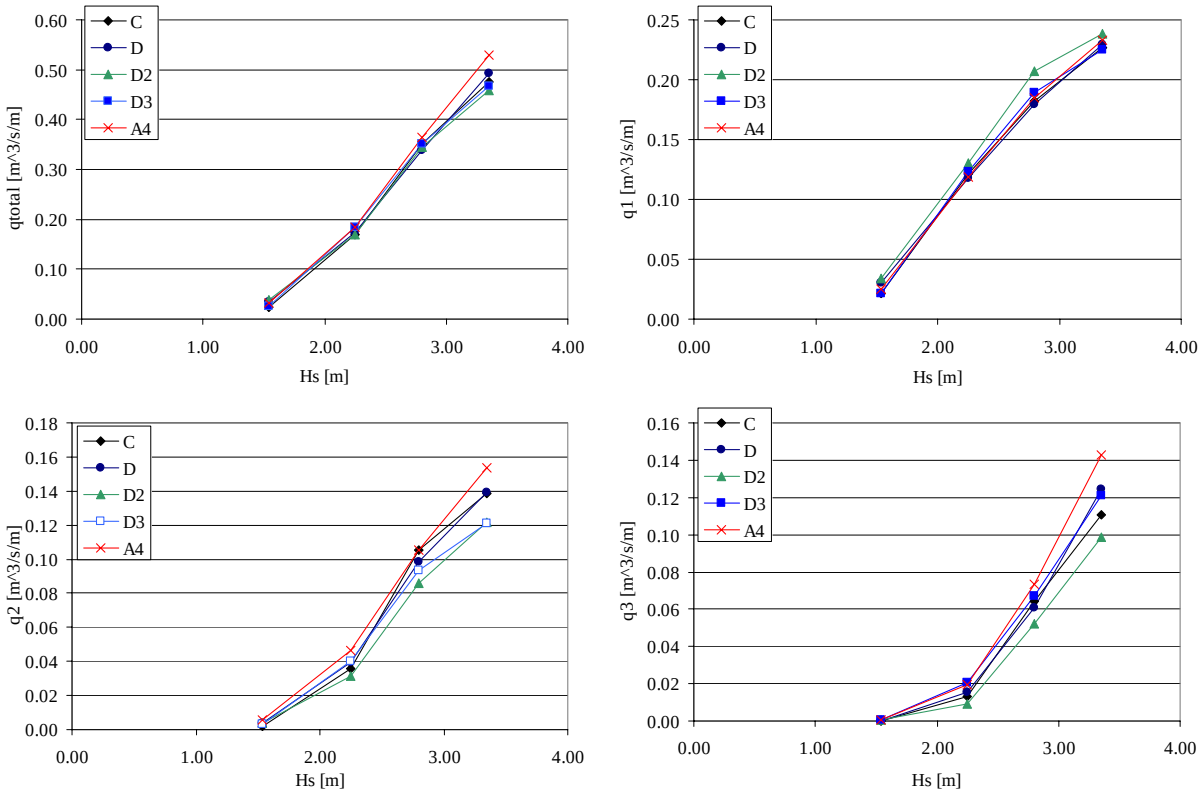

Figure 6. Geometry A4 (α = 19°), C (α = 35°), D (α = 30°), D2 (reservoir fronts cut off) and D3 (reduced horizontal distance between reservoir fronts). Upper left: Total overtopping rate as a function of wave condition. Upper right: Overtopping rate for reservoir 1 as a function of the wave condition. Lower left: Overtopping rate for reservoir 2 as a function of the wave condition. Lower right: Overtopping rate for reservoir 3 as a function of the wave condition.

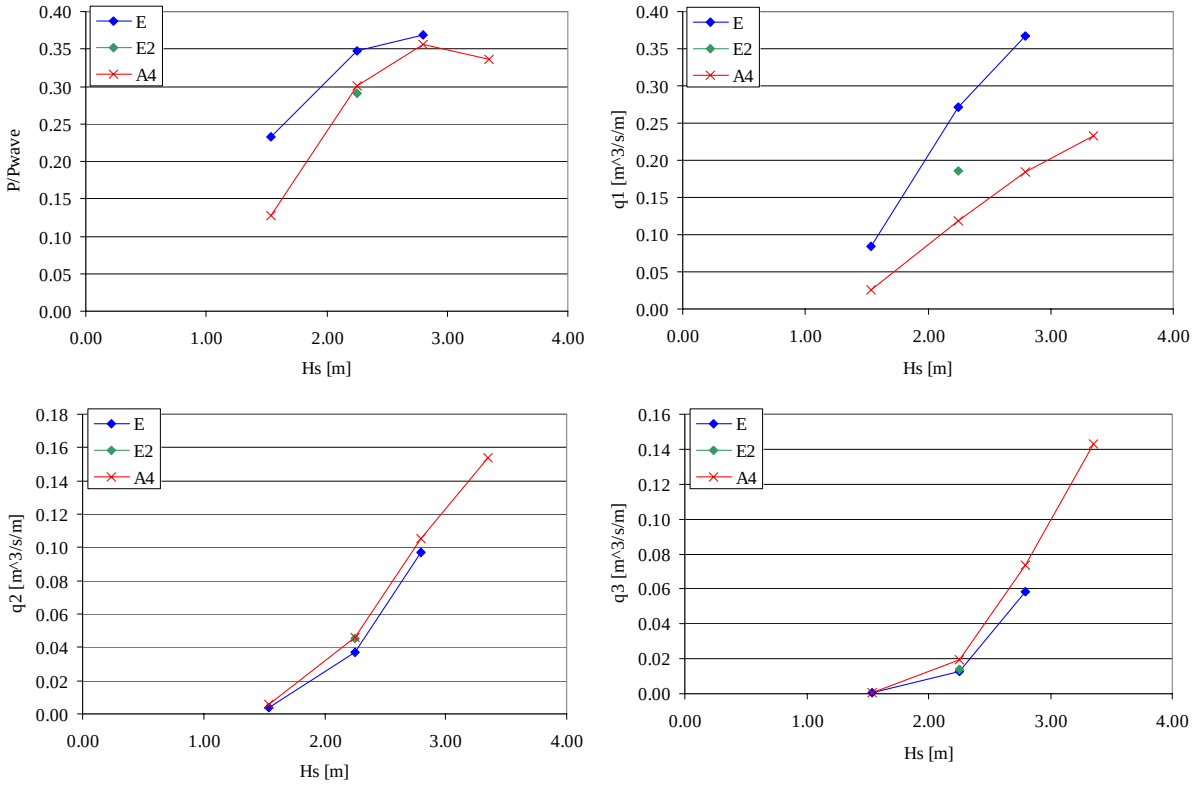

Figure 7. Geometry A4 ($R_{c,1}$ = 2.25 m), E ($R_{c,1}$ = 1.50 m) and E2 (reservoir front extended). Upper left: Total overtopping rate as a function of wave condition. Upper right: Overtopping rate for reservoir 1 as a function of the wave condition. Lower left: Overtopping rate for reservoir 2 as a function of the wave condition. Lower right: Overtopping rate for reservoir 3 as a function of the wave condition.

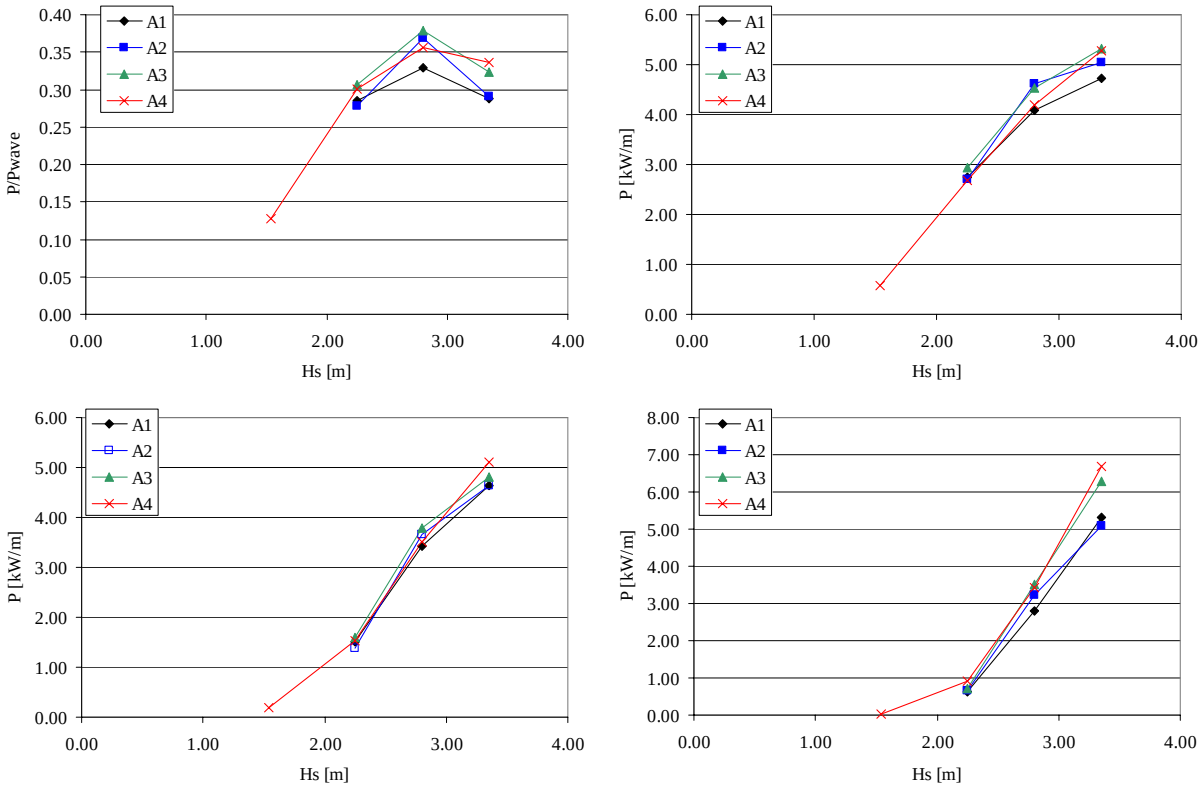

Figure 8. Geometries A1-4, length of slope in front of structure varied. Upper left: Efficiency as a function of wave condition. Upper right: Hydraulic power captured in reservoir 1 as a function of the wave condition. Lower left: Hydraulic power captured in reservoir 2 as a function of the wave condition. Lower right: Hydraulic power captured in reservoir 3 as a function of the wave condition.

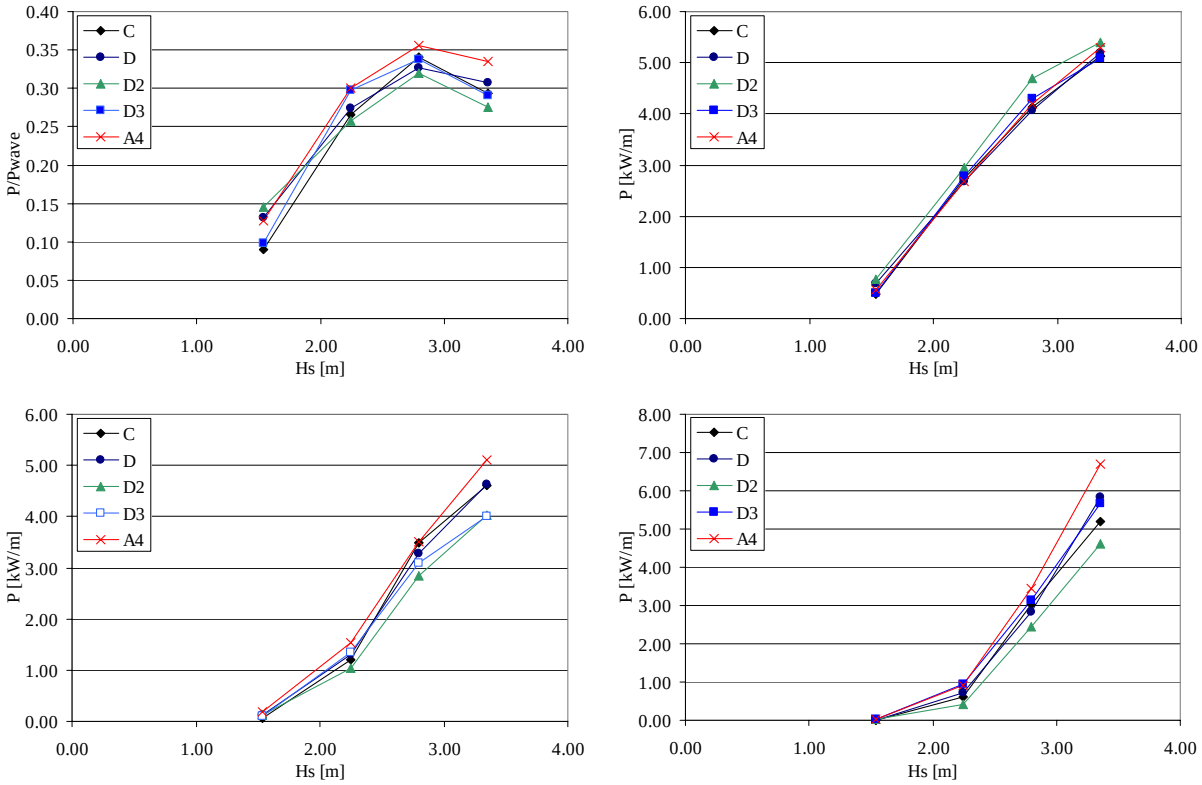

Figure 9. Geometry A4 (α = 19°), C (α = 35°), D (α = 30°), D2 (reservoir fronts cut off) and D3 (reduced horizontal distance between reservoir fronts). Upper left: Efficiency as a function of wave condition. Upper right: Hydraulic power captured in reservoir 1 as a function of the wave condition. Lower left: Hydraulic power captured in reservoir 2 as a function of the wave condition. Lower right: Hydraulic power captured in reservoir 3 as a function of the wave condition.

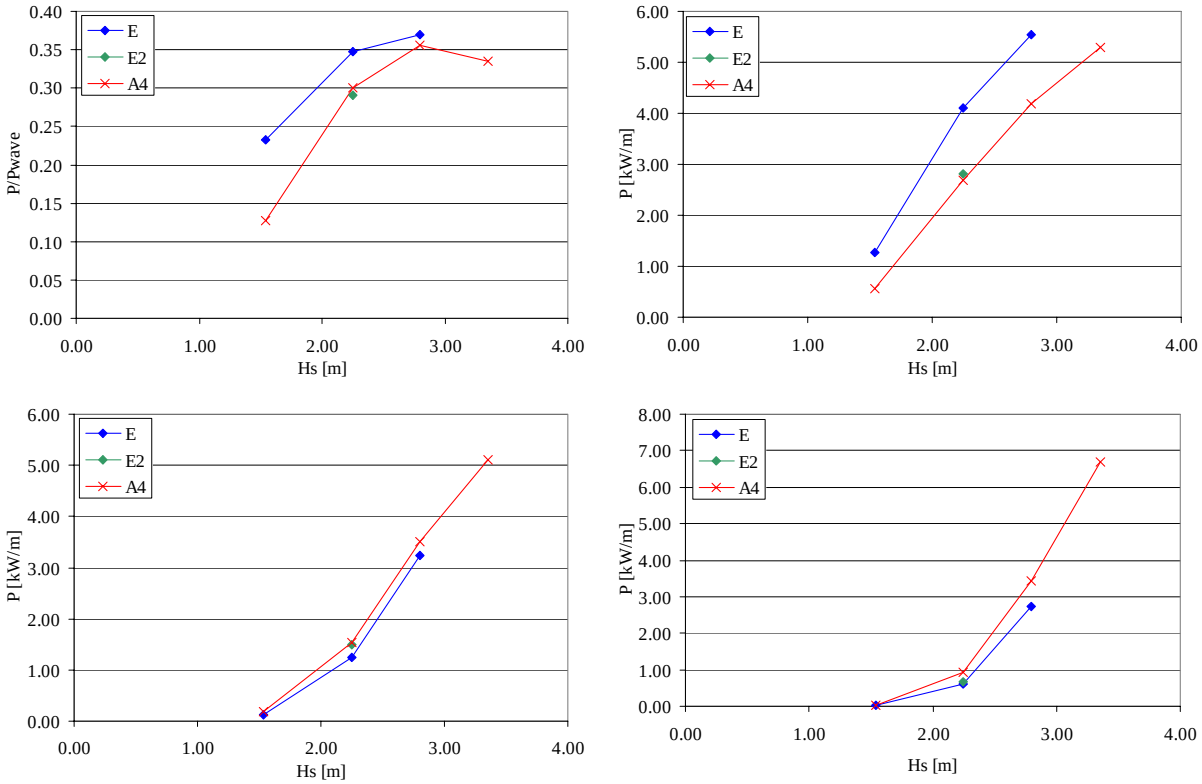

Figure 10. Geometry A4 ($R_{c,1}$ = 2.25 m), E ($R_{c,1}$ = 1.50 m) and E2 (reservoir front extended). Upper left: Efficiency as a function of wave condition. Upper right: Hydraulic power captured in reservoir 1 as a function of the wave condition. Lower left: Hydraulic power captured in reservoir 2 as a function of the wave condition. Lower right: Hydraulic power captured in reservoir 3 as a function of the wave condition.

As a check of the measured overtopping rates the total overtopping rates in all three reservoirs have been summed for the individual tests and made non-dimensional as in the overtopping expression by Kofoed (2002):

$$Q = \frac{q}{\lambda_\alpha \lambda_{d_r} \lambda_s \sqrt{gH_s}} = 0.2e^{-2.6\frac{R}{H_s}\frac{1}{\gamma_r \gamma_b \gamma_h \gamma_\beta}}$$

where

$\gamma_r = \gamma_b = \gamma_h = \gamma_\beta = 1$, corresponding to no berm, non-shallow foreshore, no roughness and head-on wave attack.

$\lambda_\alpha = \cos^3(\alpha - 30°)$, accounting for the effect of using a slope angle α different from 30°.

$\lambda_{d_r} = 1 - 0.4\frac{\sinh\left(2k_p d\left(1-\frac{d_r}{d}\right)\right) + 2k_p d\left(1-\frac{d_r}{d}\right)}{\sinh(2k_p d) + 2k_p d}$, accounting for the reduction in overtopping rates due to ramp not extending all the way to the seabed. Intended for use where the waves are allowed to pass under the structure, but has here been applied where the ramp has been cut off, leaving a vertical from the lowest point of the ramp to the seabed (geometries A1-3).

$\lambda_s = \begin{cases} 0.4\sin\left(\frac{2\pi}{3}R\right) + 0.6 & for \quad R < 0.75 \\ 1 & for \quad R \geq 0.75 \end{cases}$, accounting for low relative crest freeboards.

k_p peak wave number $2\pi/L_p$.

L_p peak wave length.

d_r draught of ramp.

R relative crest freeboard, R_c/H_s. Here set at $R_{c,1}$.

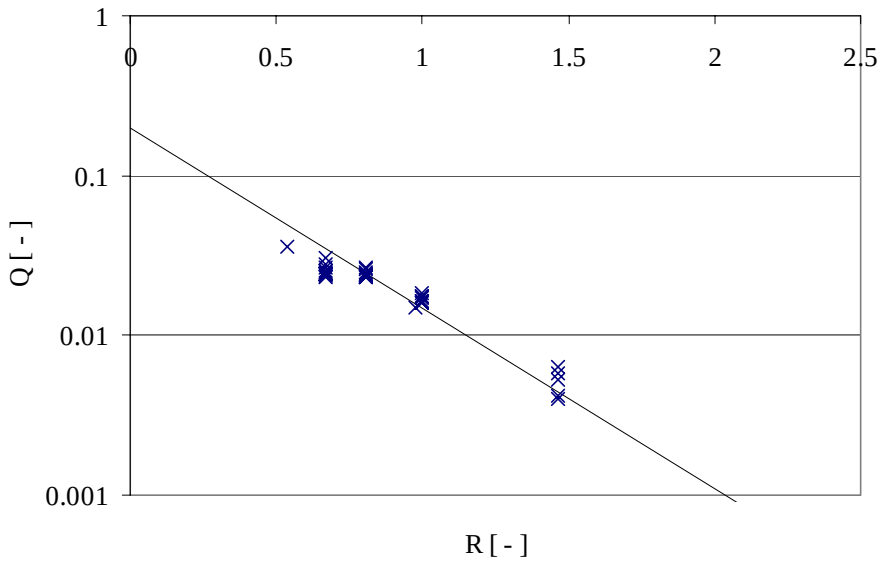

Figure 11. Non-dimensional overtopping rates as a function non-dimensional crest freeboard based on crest freeboard of the lowest reservoir. Straight line represents overtopping rate expression by Kofoed (2002).

From Figure 11 it is seen that the measured total overtopping rates in general agrees well with the overtopping expression, although a there seems to be a tendency to slight overestimation at low relative crest freeboards.

4 Interpretation of model test results

In order to enable optimization of crest freeboards for the three reservoirs data from geometry D and E has been used to determine the empirical coefficients *A*, *B* and *C* in the expression by Kofoed (2002)

$$Q' = \frac{dq/dz}{\sqrt{gH_s}} = Ae^{B\frac{z}{H_s}+C\frac{R_{c,1}}{H_s}}$$

where *Q'* is the dimensionless derivative of the overtopping discharge with respect to the vertical distance *z*.

By non-linear regression analysis the coefficients *A*, *B* and *C* has been found to be 0.197, -1.753 and -0.408, respectively. For comparison the coefficients *A*, *B* and *C* was found by Kofoed (2002) to be 0.37, -4.5 and 3.5, respectively, for model tests with reservoirs without fronts mounted.

Based on the equation above overtopping rate for individual reservoirs can be estimated using

$$\begin{aligned} q_n(z_1,z_2) &= \int_{z_1}^{z_2} dq/dz\, dz \\ &= \int_{z_1}^{z_2} \sqrt{gH_s} Ae^{B\frac{z}{H_s}} e^{C\frac{R_{c,1}}{H_s}} dz \\ &= \sqrt{gH_s^3}\frac{A}{B} e^{C\frac{R_{c,1}}{H_s}} \left(e^{B\frac{z_2}{H_s}} - e^{B\frac{z_1}{H_s}} \right) \end{aligned}$$

where z_1 and z_2 denote the lower and upper vertical boundary of the reservoir, respectively. Generally, $z_1 = R_{c,n}$ and $z_2 = R_{c,n+1}$ is used, *n* being the reservoir number. However, for the top reservoir z_2 is in principle infinite, but has here been set at 10 m (full scale).

In Figure 12 the red and green marks represents the model test results from geometry D and E, in a comparison between measured and calculated data. The straight line represents perfect agreement between measured data and the formula above.

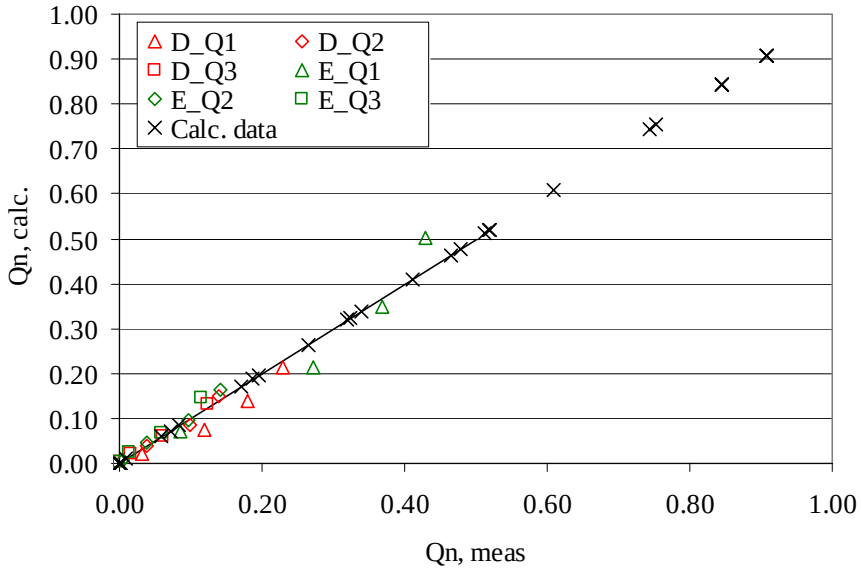

Figure 12. Comparison of calculated and measured data. The black x's represents data points found in the optimization of the crest freeboards below.

The energy contained in the overtopping water for each reservoir, called P_n, can be calculated as

$$P_n(z_1,z_2) = q_n(z_1,z_2) z_1 \rho_w g$$

and P_{total} for each wave condition can the be found as the sum of P_n of the three reservoirs.

Thus, it is possible to evaluate different crest freeboard configurations against each other by numerical calculations, and also find the optimal one in terms of maximal hydraulic efficiency for a given combination of wave conditions. This has been done for a total of four combinations of wave conditions:

- Shallow water: The four wave conditions given in Table 2, found as the realized wave conditions in the model tests.
- Shallow water, all: All ten wave conditions from Table 1, but where wave conditions 1-5 have been taken from Table 2, and H_s for wave conditions 6-10 has been roughly estimated, taking into account the local water depth. These 10 wave conditions are given in Table 6.
- Deep water: The four wave conditions covered by the range 1-5 from Table 1.
- Deep water, all: All ten wave conditions from Table 1.

Wave cond.	0-1	1-2	2-3	3-4	4-5	5-6	6-7	7-8	8-9	9-10
Hs	0.50	1.50	2.25	2.80	3.35	3.90	4.45	4.80	4.80	4.80
Tp	3.5	6.1	7.9	9.3	10.6	11.7	12.7	13.7	14.6	15.4
Prob	12.9%	30.3%	26.5%	16.4%	8.3%	3.5%	1.5%	0.5%	0.1%	0.0%
Pwave	0.4	5.9	17.1	31.1	50.9	76.1	107.6	134.9	143.8	151.7

Table 6. Roughly estimated shallow water wave conditions at prototype location.

In all numerical calculations crest levels lower than 1.5 m have been discarded, although crest levels for the lowest reservoir lower than 1.5 m is optimal, if the overall hydraulic efficiency is used as the only optimization parameter. However, a number of factors argue for not having a crest level lower than 1.5 m, among these are:

- Flow rate. For very low crest freeboards the overtopping rates are very large, demanding very large max. flow rates for the turbines. This is unlikely to be economically feasible.
- Turbine characteristics. The efficiency of the turbine is likely to be low at very low head levels.
- Vertical distance from water level in reservoir and crest level. In the calculation of the overall hydraulic efficiency the amount of energy in the overtopping water is calculated at the level of the crest. However, in reality the water level in the reservoir will only very seldom be right at the crest level and typically, say, up to 20 - 30 cm below, depending of the chosen reservoir area and turbine regulation strategy.

The numerical optimization of crest levels lead to the four results given in Table 7 to Table 11.

	Rc,1 [m]	Rc,2 [m]	Rc,3 [m]	Ptotal [kW/m]	Pwave [kW/m]	Eff.
Shallow water	1.5	2.5	4.0	5.72	15.66	0.366
Shallow water, all	1.5	2.5	4.3	7.71	20.78	0.371
Deep water	1.5	2.7	4.6	10.06	22.93	0.439
Deep water, all	1.5	2.9	5.0	14.77	33.79	0.437

Table 7. Results of the numerical optimization for the four combinations of wave conditions, given in terms of found optimal crest freeboards, average capture hydraulic power (pr. m) and overall hydralic efficiency. The underlaying data for each combination of wave conditions are given in Table 8 to Table 11.

The combinations of wave conditions called ‘shallow water’ and ‘shallow water, all’ are considered the most realistic one for the prototype location. Thus, the overall average hydraulic power in the overtopping water is expected to be 6-7 kW/m, corresponding to an overall hydraulic efficiency of 37 % for crest levels of 1.5, 2.5 and 4.0 m for the three reservoirs.

Shallow water				Rc,1 [m]	Rc,2 [m]	Rc,3 [m]		
				1.5	2.5	4.0		
Wave cond.	Q1 [m^3/s/m]	Q2 [m^3/s/m]	Q3 [m^3/s/m]	P1 [kW/m]	P2 [kW/m]	P3 [kW/m]	Ptotal [kW/m]	eff. [-]
1-2	0.0514	0.0192	0.0040	0.776	0.482	0.161	1.42	0.241
2-3	0.1521	0.0889	0.0397	2.297	2.236	1.597	6.13	0.359
3-4	0.2409	0.1685	0.1055	3.637	4.240	4.249	12.13	0.389
4-5	0.3344	0.2646	0.2124	5.050	6.658	8.551	20.26	0.398

Table 8. Optimal crest freeboards found from the numerical optimization using the 'shallow water' combination of wave conditions, in terms of overtopping rates, resulting hydraulic power and hydraulic efficiency for the individual wave conditions.

Shallow water, all				Rc,1 [m]	Rc,2 [m]	Rc,3 [m]		
				1.5	2.5	4.3		
Wave cond.	Q1 [m^3/s/m]	Q2 [m^3/s/m]	Q3 [m^3/s/m]	P1 [kW/m]	P2 [kW/m]	P3 [kW/m]	Ptotal [kW/m]	eff. [-]
0-1	0.0002	0.0000	0.0000	0.003	0.000	0.000	0.00	0.008
1-2	0.0514	0.0203	0.0028	0.776	0.512	0.122	1.41	0.240
2-3	0.1521	0.0972	0.0313	2.297	2.446	1.356	6.10	0.357
3-4	0.2409	0.1870	0.0870	3.637	4.706	3.767	12.11	0.389
4-5	0.3344	0.2968	0.1801	5.050	7.469	7.797	20.32	0.399
5-6	0.4278	0.4183	0.3099	6.460	10.525	13.414	30.40	0.399
6-7	0.5197	0.5468	0.4738	7.846	13.759	20.505	42.11	0.392
7-8	0.5767	0.6303	0.5934	8.707	15.861	25.684	50.25	0.372
8-9	0.5767	0.6303	0.5934	8.707	15.861	25.684	50.25	0.349
9-10	0.5767	0.6303	0.5934	8.707	15.861	25.684	50.25	0.331

Table 9. Optimal crest freeboards found from the numerical optimization using the 'shallow water, all' combination of wave conditions, in terms of overtopping rates, resulting hydraulic power and hydraulic efficiency for the individual wave conditions.

Deep water				Rc,1 [m]	Rc,2 [m]	Rc,3 [m]		
				1.5	2.7	4.6		
Wave cond.	Q1 [m^3/s/m]	Q2 [m^3/s/m]	Q3 [m^3/s/m]	P1 [kW/m]	P2 [kW/m]	P3 [kW/m]	Ptotal [kW/m]	eff. [-]
1-2	0.0562	0.0163	0.0020	0.849	0.444	0.092	1.38	0.236
2-3	0.2166	0.1208	0.0423	3.270	3.283	1.959	8.51	0.405
3-4	0.4126	0.3074	0.1804	6.229	8.354	8.353	22.94	0.470
4-5	0.6108	0.5360	0.4293	9.222	14.567	19.876	43.67	0.478

Table 10. Optimal crest freeboards found from the numerical optimization using the 'deep water' combination of wave conditions, in terms of overtopping rates, resulting hydraulic power and hydraulic efficiency for the individual wave conditions.

Deep water, all				Rc,1 [m]	Rc,2 [m]	Rc,3 [m]		
				1.5	2.9	5.0		
Wave cond.	Q1 [m^3/s/m]	Q2 [m^3/s/m]	Q3 [m^3/s/m]	P1 [kW/m]	P2 [kW/m]	P3 [kW/m]	Ptotal [kW/m]	eff. [-]
0-1	0.0002	0.0000	0.0000	0.003	0.000	0.000	0.00	0.008
1-2	0.0600	0.0133	0.0012	0.906	0.387	0.063	1.36	0.231
2-3	0.2380	0.1099	0.0317	3.594	3.208	1.597	8.40	0.399
3-4	0.4603	0.2948	0.1453	6.950	8.604	7.313	22.87	0.469
4-5	0.6876	0.5297	0.3587	10.382	15.463	18.054	43.90	0.480
5-6	0.9069	0.7869	0.6580	13.693	22.969	33.114	69.78	0.462
6-7	1.1146	1.0506	1.0210	16.828	30.668	51.385	98.88	0.431
7-8	1.3103	1.3129	1.4279	19.783	38.323	71.864	129.97	0.396
8-9	1.4947	1.5696	1.8632	22.567	45.816	93.769	162.15	0.362
9-10	1.6689	1.8188	2.3154	25.198	53.091	116.530	194.82	0.329

Table 11. Optimal crest freeboards found from the numerical optimization using the 'deep water, all' combination of wave conditions, in terms of overtopping rates, resulting hydraulic power and hydraulic efficiency for the individual wave conditions.

In order to utilize as much of the available hydraulic power in the overtopping water as possible it is important to dimension the reservoirs, the turbine(s) and the control system for the turbine(s) appropriately. In this connection the following items are of importance:

- The average vertical distance between the water levels in the individual reservoirs and the corresponding crest levels should be controlled so it does not get un-necessarily large, as it directly leads to loss of power, but it should not be too small, as loss of power due to spilling then will occur. Here the area of the reservoirs, the turbine capacity, and the control strategy all plays a role.

- The capacity of the turbine(s) needs to be adjusted for the individual reservoirs to allow for the handling of the occurring flow rates. Here it should be noticed that the overtopping rates given in Table 7 to Table 11 are averages, and the need turbine capacity will need to be considerably larger than the here given values if all the available hydraulic power is to be utilized. However, it will most probably not be economically feasible to dimension the turbine(s) so it can handle all water in all conditions.

The above mentioned items will to some extend decrease the power available to the turbine compared to the stated hydraulic power.

5 Conclusions

From an examination of the results presented in Chapter 3 the following conclusion have been drawn:

- From the results of the tests with geometries A1-4 it is seen that best performance is obtained with the slope in front of the structure extending to or close to the bottom. Actually, A3 shows a slightly better performance than A4, which is not expected, if looking at e.g. the definition of λ_{dr}. which goes towards 1 in a monotone manner for increasing d_r. However, one explanation hereof can be that the slope angle of 19° is so gentle that when the slope is extending all the way to the bottom wave breaking is tricked by the slope.
- From the results of the tests with geometries A4, C and D, where slope angles of 19°, 35° and 30° were tested, it was found that the slope angle results in the best performance. This is in contradiction with findings for single level reservoirs in the literature, see Kofoed, 2002, where the optimal slope angle is found and quoted to be in the 30° - 40° range. The present test thus indicates that the situation is different when utilizing multiple reservoirs.
- From the results of the tests with geometries D and D2, where the fronts on reservoir 2 and 3 were cut off at the crest level of reservoir below in the later, it is seen that the cutting off of the fronts decrease the performance a little. However, in the case where the crest level of reservoir 1 is lowered to 1.50 m instead of 2.25 m (geometries E2 and E) it is found that extending the front below the crest level of the reservoir below has a blocking effect, because of the increased overtopping rate in reservoir 1, due to the lower crest freeboard. This indicates that the extension of the fronts below the crest of the reservoir below is reasonable, but it is a balance. The extension can cause an unwanted blocking for the water getting into the reservoir below in larger wave conditions, which then leads to a decrease in performance.
- From the results of the tests with geometries D2 and D3, where the horizontal distances between reservoirs have been reduced in the later, shows an increased performance for the reduced distances. Obviously, there is a limit to how much the distances can be reduced as at some point the intake capacity of the lowest two levels will be reduced so much that it will result in loss of overtopping.
- From the results of the tests with geometries D and E, where $R_{c,1}$ is reduced from 2.25 m to 1.5 m in the later, a very significant increase in the overall performance is found. Due to too large amounts of overtopping (for the overtopping measuring setup) in the lowest reservoir in case of the reduced crest freeboard, a test with wave condition 4-5 for geometry E was not performed. However, from a realistic extrapolation of the measured efficiencies for geometry E, and comparison with the tests with the other geometries, it is estimated that the efficiency of geometry E in wave condition 4-5 would around 0.35. In this case the overall efficiency based on wave conditions 1-5 would be 0.342, which is 21 % more than geometry D (0.283, see Table 5).

From the numerical optimizations described in Chapter 4 the following is concluded:

- For the combination of wave conditions considered the most realistic (called ‘shallow water, all) the overall average hydraulic power in the overtopping water is expected to be 6-7 kW/m corresponding to an overall hydraulic efficiency of 37 % for crest levels of 1.5, 2.5 and 4.0 m for the three reservoirs.
- Not all of the hydraulic power in the overtopping water will be available for the turbine(s), as there will always be a level difference between the water and crest in each of the individual reservoirs, and it will most probably not be feasible to install turbine capacity to avoid overflow in all conditions.

6 Recommendations

Based on the experiences reported above the following recommendations are given (in prioritized order):

- In order to provide a more realistic combination of wave conditions at the location of the prototype, transformation of waves from offshore to location is needed. This can be done numerical modeling using a model like MildSim developed at AAU (see http://www.hydrosoft.civil.auc.dk/).
- Further crest freeboard optimization, including checking/verification of results from the numerical optimization by physical model tests. Once more detailed turbine performance curves are available these can also be incorporated in the optimization by calculations.
- Further model testing with slope angles in the 20° - 30° ranges would be appropriate.
- Model testing of the influence of the horizontal distances between reservoirs crests and angles of reservoir fronts. However, the number of possible combinations is large and the effect is most probably limited. Therefore, it is recommended to look in Kofoed, 2002b, pick a few reasonable designs, and then performed a limited number of model tests.
- As the structure is fixed to the seabed the influence of the local tide variations on the overtopping, turbine performance, and thus the power production needs to be considered. To do this statistical data on the local tide variations is needed.

Based on the practical experiences during the performed model tests the demanded overtopping measurement capacity needs to be decreased in the test setup when tests with lower crest freeboards are to be performed. This can be achieved by reduction of reservoir width or model size, or more pipes and pumps.

7 Literature

DS 449 (1983): *DS 449. Dansk Ingeniørforenings norm for pælefunderede offshore stålkonstruktioner*. 1. udg. april 1983.

Falnes, J. (1993): *Theory for extraction of ocean wave energy*. Division of Physics, Norwegian Institute of Technology, University of Trondheim, Norway, 1993.

Kofoed J. P. (2002): *Wave Overtopping of Marine Structures – Utilization of Wave Energy*. Ph. D. Thesis, defended January 17, 2003 at Aalborg University. Hydraulics & Coastal Engineering Laboratory, Department of Civil Engineering, Aalborg University, December, 2002.

Kofoed, J. P. (2002b): *Hydrauliske undersøgelser af bølgeenergianlægget Power Pyramid – fase 2*. Hydraulics & Coastal Engineering Laboratory, Aalborg University, October 2002. In Danish. (Title in english: Hydraulic investigations of the wave power device Power Pyramid – phase 2.)

Kofoed, J. P. (2004), Frigaard, P., Friis-Madsen, E. and Sørensen, H. C.: *Prototype testing of the wave energy converter Wave Dragon*. 8th. World Renewable Energy Congress, Denver, USA, Sept. 2004.

Torsethaugen, K. (1990): *Bølgedata for vurdering av bølgekraft*, SINTEF NHL-report No. STF60-A90120, 1990-12-20, ISBN Nr. 82-595-6287-1.

Vind- og temperaturstatistikk, DNMI.